XLVI CILAMCE
VITÓRIA - ES - BRAZIL - 2025
XLVI IBERO-LATIN AMERICAN CONGRESS ON COMPUTATIONAL METHODS IN ENGINEERING

Estimating free-fluid porosity from microtomography image erosion: A case study of coquinas from the Morro do Chaves Formation

BERMUDEZ, S.L.B.[1]; RIBEIRO, G.S.S.[1]; PINEIRO, T.[1]; GUEDES, L.B.[1]; BOYD, A.[1]; LIMA, M.C.O.[1]; ALVES, J.L.D.[2]; COUTO, P.[1]

[1]*LRAP+, Program of Civil Engineering, Federal University of Rio de Janeiro, Brazil,* silviabermudez@petroleo.ufrj.br, gabriel.ribeiro@petroleo.ufrj.br, thiago.pineiro@petroleo.ufrj.br, luciano.guedes@petroleo.ufrj.br, austin@petroleo.ufrj.br, maira.lima@petroleo.ufrj.br, pcouto@petroleo.ufrj.br
[2]*LAMCE, Program of Civil Engineering, Federal University of Rio de Janeiro, Brazil,* jalves@lamce.coppe.ufrj.br
Avenida Moniz Aragão, 360 - BL4 Cidade Universitária, 21941594, Rio de Janeiro, Brazil

Abstract. Free fluid porosity (FFI) is a crucial petrophysical parameter in reservoir characterization, representing the porous fraction with potentially producible fluids. Traditionally, the distribution of transverse relaxation times (T_2) obtained by Nuclear Magnetic Resonance (NMR) is used to estimate the presence of mobile fluids, with a cutoff value ($T_{2cutoff}$) separating mobile fluids from irreducible fluids retained by capillary forces or adsorption. This estimate is particularly relevant in hybrid carbonate reservoirs with mixed facies, where conventional NMR interpretation has limitations. This study proposes an innovative approach to estimate FFI through digital erosion of segmented images obtained by microtomography (microCT). For the case study, coquinas from the Morro do Chaves Formation (Sergipe-Alagoas Basin) were analyzed and considered analogous to the Pre-Salt reservoirs. Six samples were subjected to petrophysical, NMR, MICP, and microCT analyses. The segmented images, previously centrifuged, allowed the estimation of $T_{2cutoff}$. The FFI derived from microCT was used as input in the Timur-Coates model, and the results were compared with permeabilities measured by routine core analysis. The microCT model showed good correlation ($R^2 = 0.686$; $r = 0.839$; $\sigma_k = 0.408$), comparable to the NMR-based model ($R^2 = 0.756$; $r = 0.863$; $\sigma_k = 0.368$), validating the method as a robust and non-destructive alternative for petrophysical characterization in heterogeneous carbonate rocks.

Keywords: Free fluid porosity (FFI), Nuclear Magnetic Resonance (NMR), Computerized Microtomography (microCT), Hybrid Carbonates, Timur-Coates model permeabilities.

1 Introduction

The petrophysical characterization of reservoirs is an essential step for efficiently evaluating and developing hydrocarbon resources. Among the critical parameters used in this process, free fluid porosity (FFI) stands out, representing the fraction of the porous volume occupied by potentially producible fluids [1-3]. FFI is directly related to the productivity of a reservoir and is fundamental for estimating recoverable volumes of oil and gas. Traditionally, FFI is determined from Nuclear Magnetic Resonance (NMR) measurements, based on the distribution of transverse relaxation times (T_2). The technique uses a cutoff value ($T_{2cutoff}$) to separate mobile fluids—associated with larger pores—from irreducible ones, retained in micropores due to capillary forces or adsorption on mineral surfaces [4].

Despite the effectiveness of NMR in various geological contexts, its application in hybrid carbonate rocks, which have mixed siliciclastic and carbonate facies, may be limited by the textural complexity and variability of the porosity systems present [5]. In this scenario, alternative approaches that integrate different data types have been explored to overcome the limitations of conventional methods. Among them, X-ray computed microtomography (microCT) stands out as a non-destructive imaging technique capable of providing high-resolution three-dimensional information about the structure of the pore space. These images' segmentation and

digital processing allow petrophysical properties to be quantified and extracted directly from the pore geometry. This work proposes an innovative approach for estimating FFI from segmented microCT images, applying the digital erosion technique to distinguish regions of porosity associated with free fluids. As a case study, coquinas from the Morro do Chaves Formation, located in the Sergipe-Alagoas Basin, represent an example of hybrid carbonate rock. The Sergipe-Alagoas Basin is located in northeastern Brazil, covering an area of approximately 32,760 km², extending approximately 350 km in length and 20–50 km in width. The Morro do Chaves Formation, of Jiquié age, consists of carbonate successions with a thickness of 50–350 m, composed mainly of coquinas interbedded with siliciclastic rocks from the Coqueiro Seco and Rio Pitanga formations [6,7]. Diagenetic processes, such as neomorphism, compaction, and micritization, significantly modified the pore systems of these rocks, leading to the preservation of primary porosity, the creation of secondary porosity, and the obliteration of pores, resulting in heterogeneous porosity and permeability [8], which makes this formation an excellent analogue to Brazilian Pre-Salt reservoir rocks.

The FFI derived from microCT images is integrated into the empirical permeability model developed by Timur-Coates [4] and compared to permeability measurements obtained by gas flow and estimates based on NMR data. The proposed approach aims to contribute to high-resolution petrophysical characterization and more accurate modeling of complex porous media, offering an alternative, robust, and non-destructive workflow for applications in unconventional reservoirs with high lithological heterogeneity.

2 Materials and Methods

Six coquina core plugs (2.5 cm in diameter and 5 cm in height) were collected from well 02-SMC-02 at the Atol Quarry in São Miguel dos Campos, Alagoas (Brazil). The samples were cleaned using the Soxhlet method (toluene and methanol), dried at 60 °C with 40% humidity for 24 hours, and subsequently analyzed by routine core analysis (RCAL) to obtain porosity and permeability, based on Boyle's law and Darcy's law. These values served as a reference for comparison with NMR-derived data. For the NMR analysis, samples were saturated with KCl brine (30,000 ppm, 1.0167 g/cm³) under 2000 psi for 24 hours, reaching saturation above 95%. Measurements were performed using a 2 MHz Geospec instrument, employing the Carr-Purcell-Meiboom-Gill (CPMG) pulse sequence. T_2 distributions were obtained through inverse Laplace transform using LithoMetrix™ software. After centrifugation to remove free water, the samples were remeasured under irreducible water saturation (S_{wir}) conditions via NMR. From these data, T_2 cutoff values, porosity, free fluid index (FFI), bound volume irreducible (BVI), and permeability via NMR were calculated.

In NMR techniques, total porosity (ϕ_{NMR}) is divided into two components based on the $T_{2cutoff}$ value: bound volume irreducible (BVI), corresponding to fluid retained by capillary forces, and free fluid index (FFI), associated with movable and potentially producible fluids. Small pores are generally assumed to contain irreducible water, while larger pores host mobile fluids (water or hydrocarbons). These parameters enable the evaluation of fluid mobility within the pore network and the distinction between producible and retained fluids in the reservoir. BVI represents the pore fraction occupied by immobile fluids—typically irreducible water—that remains adhered to the rock matrix due to capillary and surface forces. These fluids are concentrated in smaller pores, where capillary pressure exceeds the formation pressure, preventing displacement. The FFI/BVI ratio is commonly used as a qualitative indicator of the reservoir's producibility potential. The total porosity from NMR is expressed by eq. 1:

$$\emptyset_{NMR} = BVI + FFI \tag{1}$$

when a rock is fully saturated with water, the T_2 value of a single pore is proportional to the surface area/volume ratio (S/V) of the pore, which is a measure of pore size. Thus, the observed T_2 distribution of all pores in the rock represents the pore size distribution of the rock. At the limit of the fast diffusion regime, the T_2 time of a fluid saturating a porous medium is given by (eq. 2):

$$\left(\frac{V}{S}\right)_{pore} = \rho_2 T_2 \tag{2}$$

where ρ_2 represents the surface relaxivity, this equation shows that the relaxation times of fluids within the pores are inversely proportional to the surface-to-volume ratio (S/V) of the pores, with the scale of this relationship defined by the surface relaxivity, ρ_2.

MICP tests were performed using an Autopore IV 9500 (Micromeritics Instruments Co.) on subsamples adjacent to the core plugs, due to the destructive nature of the technique. The method involves injecting mercury under progressively increasing pressure, allowing estimation of the relationship between capillary pressure and

pore volume, initially invading the larger pores. Assuming cylindrical pore geometry, the Washburn equation [9] relates the applied pressure to the pore throat radius.

The NMR T_2 distribution was integrated with the MICP data to estimate surface relaxivity (ρ_2), enabling calibration of the T_2 curves to represent pore size distributions. Equation 2 allows conversion of T_2 values into pore radii by considering the geometric shape of the pores [10]. The effective relaxivity (ρ_e) is adjusted to align the NMR-derived distributions (which are sensitive to pore volume) with the MICP-derived distributions (which are sensitive to pore throats), using eq. 3.

$$\left(\frac{S}{V}\right)_{cylinder} = \frac{2\pi r l}{\pi r^2 l} = \frac{2}{r} \quad \rightarrow \quad r_{cylinder} = 2\rho_e T_2 \tag{3}$$

where l is the length of the cylinder. The value 2 is valid for cylindrical pores, and it is necessary to convert the surface-to-volume ratio (S/V) in eq. (2) into pore throat radii. The combination of NMR and MICP measurements will not yield reliable results unless there is a correlation between the pore size distribution curves and the corresponding pore throat distributions [11].

The methodology described above for converting T_2 values into pore radii was applied to determine the $T_{2cutoff}$ in terms of pore radius, thereby enabling an estimation of this value at the resolution of the microCT images. The microCT images were acquired with a pixel size of 14 µm, meaning that the entire portion of the pore size distribution curve below 7 µm (half the pixel size, corresponding to the pore radius) is considered sub-resolution and therefore not visible. Consequently, all pores in the curve above this value can be visualized at this resolution. The porosity of the region detectable by resolution—that is, the distinguishable fraction of solid rock material—corresponds to the total area under the NMR curve, from the smallest pore radius resolvable by the image to the distribution limit. Thus, the maximum porosity value that can be seen in microCT images at a given resolution is defined by the NMR, which helps to choose the ideal threshold value for calculating the porosity of the image.

To determine the porosity of microCT data, the commercial software Avizo was used, and six image stacks from different plugs were submitted to a multi-phase segmentation by a watershed module and then processed through arithmetic operations to quantify sub-resolution porosity in a multi-step workflow. In the first step, the gradient magnitude was thresholded (i.e., the region of transition between the voxel intensities in the image stack) to mark the edges between phases. Next, five phases were thresholded for each one stack: resolved pores, sub-resolution pore space, solids, high attenuation, and the external portion that involves the plug. Since the watershed segmentation could generate a multi-phase map with five regions (corresponding to the previous thresholded phases), it was possible to mask the original stack and to extract the intensity values from the voxels that are related to the solid and resolved pores regions in the multi-phase map. With this, the sub-resolution pore space from the original image stack was estimated by arithmetic calculations that demand both a multi-phase segmented map and the original stack as input. The estimation was based on Foroughi et al, 2024 [12], eq. 4.

$$\bar{I}_{dry} = \emptyset\, I_{air} + (1 - \emptyset) I_{rock} \tag{4}$$

where $\bar{I}_{dry}$ represents the average intensity of a single voxel, in the context of dry-scan images, while I_{air} and I_{rock} are associated with intensities of the saturating air and the rocky component of the considered voxel. In this case, the intensity values of air and rock were obtained from the extraction using the masking approach above. At the same time, arithmetic operations provided the average intensity of the voxels. A new image with pore percent for each voxel was then generated, and the porosity was estimated by the average porosity obtained by voxel counting.

Finally, to get the FFI, an erosion step was performed in all volumes of this new image, except in the voxels characterized as 100% pore percent. The erosion tool in image processing consists of removing pixels from the edges of an object in binary images. In this way, the selected region that does not contain the FFI is reduced by a defined number of voxels [13]. In this study, the erosion of one voxel was used. The goal of applying this technique is to isolate the free fluid portions of the image that would be associated not only with resolved pore space, but also with transition zones (gradient voxels) that are marked with sub-resolution porosity. The eroded portion, on the other hand, may define the BVI zone in this new image.

In the empirical Free Fluid or Timur-Coates (TC) model, permeability (k) is estimated based on the porosity derived from NMR measurements, considering the division of fluids into movable and irreducible phases. The model is founded on a direct correlation between permeability and the volume of free fluid, and an inverse correlation with the volume of irreducible fluid (eq. 5).

$$k_{NMR} = C \left(\frac{FFI_{NMR}}{BVI_{NMR}}\right)^a \emptyset_{NMR}^b \tag{5}$$

where k is the permeability, ϕ is the total NMR porosity, FFI is the free fluid volume (typically with $T_2 > T_{2cutoff}$), BVI is the bound or immobile fluid volume (typically with $T_2 < T_{2cutoff}$), and C is an empirical constant determined through calibration with core measurements [14].

This study proposes a method to estimate free fluid porosity (FFI) from microCT images using a digital erosion operation on segmented pore images. MicroCT provides a porosity map from which a value of FFI can be derived that is proportional to the image resolution. Based on the $T_{2cutoff}$ fraction determined by eq. 3, we estimate the corresponding pore radius detectable by microCT resolution. From this, we calculate the percentage of FFI visible in the images and, through proportional weighting, estimate the total FFI ($FFI_{\mu CT}$). Knowing the total porosity obtained from microCT ($\phi_{\mu CT}$), it is possible to estimate the irreducible fluid porosity ($BVI_{\mu CT}$), and subsequently apply eq. 5, adapted to microCT data, resulting in eq. 6.

$$k_{\mu CT} = C \left(\frac{FFI_{\mu CT}}{BVI_{\mu CT}}\right)^{a} \emptyset_{\mu CT}^{b} \tag{6}$$

3 Results and Discussion

Table 1 presents the results of the RCAL, including porosity and permeability, as well as the porosity values obtained from NMR and microCT, the $T_{2cutoff}$ values converted to micrometers (μm), the estimated ρ_e values for each sample, and the FFI values (in percentage) estimated via NMR and microCT. The porosities measured by routine analysis ranged from 8.7% to 20.19%, while permeabilities ranged from 4.32 to 243.58 mD. The estimated $FFI_{\mu CT}$ values were generally close to the corresponding FFI_{NMR} values, except for sample 170.65, where the difference was significantly higher. The porosity obtained from NMR showed a strong correlation with routine porosity, with a coefficient of determination of $R^2 = 0.977$, indicating that the results were consistent and that the samples were properly saturated. Similarly, the porosity results from microCT, derived from the porosity map calibrated with routine analysis data, also showed excellent correlation ($R^2 = 0.996$). These results demonstrate that eq. 1 can be applied to microCT data in a viable and reliable manner.

Table 1. Petrophysical properties of the analyzed samples, including gas porosity (ϕ_{N2}), gas permeability (k_{N2}), porosity estimated from NMR (ϕ_{NMR}) and micro-CT ($\phi_{\mu CT}$), $T_{2cutoff}$ values, and ρ_e relaxation parameters and values of FFI via NMR and microCT.

Samples	ϕ_{N2} **(%)**	k_{N2} **(mD)**	ϕ_{NMR} **(%)**	$\phi_{\mu CT}$ **(%)**	$T_{2cutoff}$ **(μm)**	ρ_e **(μm/s)**	FFI_{NMR} **(%)**	$FFI_{\mu CT}$ **(%)**
73.20	18.18	68.30	17.7	16.7	1.604	9	14.72	11.06
88.00	8.7	4.81	9.0	8.2	0.505	4	6.04	9.70
93.00	19.77	226.97	17.9	18.7	4.389	11	13.43	12.95
141.00	11.8	4.32	11.1	10.9	6.200	11	7.21	7.03
170.65	20.19	243.58	20.1	19.4	1.403	14	13.65	5.06
187.95	12.14	107.63	12.4	11.1	2.818	5	8.99	7.13

Figure 1 shows the pore throat size distributions from MICP and NMR (converted to pore radius) for samples 141.0 and 170.65. MICP highlights the initial mercury intrusion into larger pores, while NMR displays broader distributions due to its sensitivity to both pore bodies and throats. After visually confirming the strong correlation between the mercury saturation and T_2 distributions, we calibrated the parameter ρ_e in eq. (3) until both curves showed the same maximum peak, as illustrated in Fig. 1. The vertical lines indicate the $T_{2cutoff}$ value (purple) and the microCT resolution limit (green).

Sample 141.0 has the lowest permeability in the set and exhibits a bimodal T_2 distribution, with peaks in the micro- and mesopore regions. The pore partitions of Silva et al. (2015) [15] were considered. MICP analysis revealed reduced radius throats, consistent with its low permeability. There is good agreement between the NMR and MICP curves in the mesopore region. The $T_{2cutoff}$ lies near the microCT resolution limit, suggesting that the imaging can potentially resolve most pores associated with free fluids. Sample 170.65 exhibits the highest permeability in the set and shows a more pronounced bimodal T_2 distribution, with characteristic peaks of micro- and mesopores. The MICP curve behaves similarly to NMR in both regions. An increase in the pore space of the microporous region and higher pore throat values can be observed, consistent with the higher permeability and porosity values. The $T_{2cutoff}$ value of 1.4 μm, located near the first mode of the distribution, indicates the

coexistence of pores with different fluid mobilities. This distinction is essential for interpreting flow behavior: larger pores contribute predominantly to permeability, while smaller pores are responsible for storage. The $T_{2cutoff}$ value suggests that pores associated with mobile fluids will be only partially resolved by microCT.

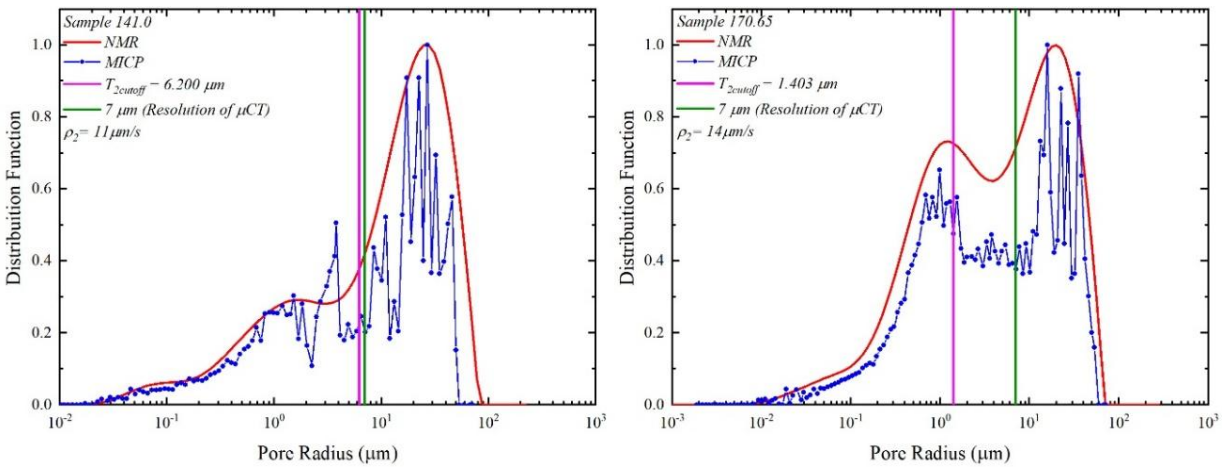


Figure 1. Comparison of pore throat size distributions obtained from MICP (blue curves) and fitted NMR data (red curves) for 141.0 and 170.65 samples. The purple vertical lines indicate the $T_{2cutoff}$ values, and the green vertical lines correspond to the microCT resolution limit (7 μm).

For example, Fig. 2 shows a segment of sample 141.0, in which the free-fluid porosity (FFI) was estimated by applying digital erosion to the images with pore percent. Figure 2a represents a pore percent image. Figure 2b shows the original pore segmentation, including regions with total porosity and transitional zones with partial porosity, which are potentially associated with sub-resolution pores. In Figure 2c, the erosion was applied to all voxels except those classified as 100% porous. The main objective of this operation is to isolate the volume corresponding to FFI more accurately by removing edge voxels with gradient transitions. Therefore, the resulting eroded region can be associated with the volume of irreducible fluid (BVI) in the image. This technique enables a more apparent spatial distinction between the volumes related to FFI and BVI based on the pore geometry observed in the microCT images.

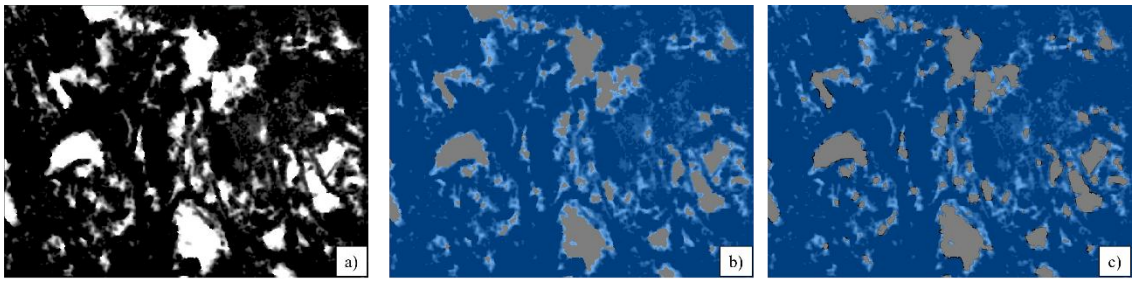


Figure 2. Pore segmentation from a microCT zoom of sample 141.0. a) pore percent image; before (b) and after (c) digital erosion.

Figure 3 presents a microCT slice of sample 141.0, acquired with a voxel size of 14 μm, illustrating the image processing steps used to characterize porosity and the free fluid space (FFI) in the rock. Image (Fig. 3a) shows the original grayscale slice (16-bit), where pores appear in black and the rock matrix in shades of gray, serving as the basis for segmentation processes. In image (Fig. 3b), a region map generated through multiphase segmentation is displayed: light blue represents directly resolved pores, dark blue indicates areas of sub-resolution porosity (smaller than the voxel size), and red corresponds to solid rock material. Image (Fig. 3c) assigns a porosity value to each voxel, where white tones represent voxels with 100% porosity, lighter gray tones indicate higher porosity percentages, darker tones indicate lower porosity, and black marks voxels with no porosity (0%). Finally, Fig. 3d, shows the FFI space estimated through a digital erosion operation, applied to remove regions associated with solids and voxels with porosity below 100%. This step isolates the portion of the pore space potentially

occupied by movable fluids, providing a more accurate spatial representation of FFI within the porous medium.

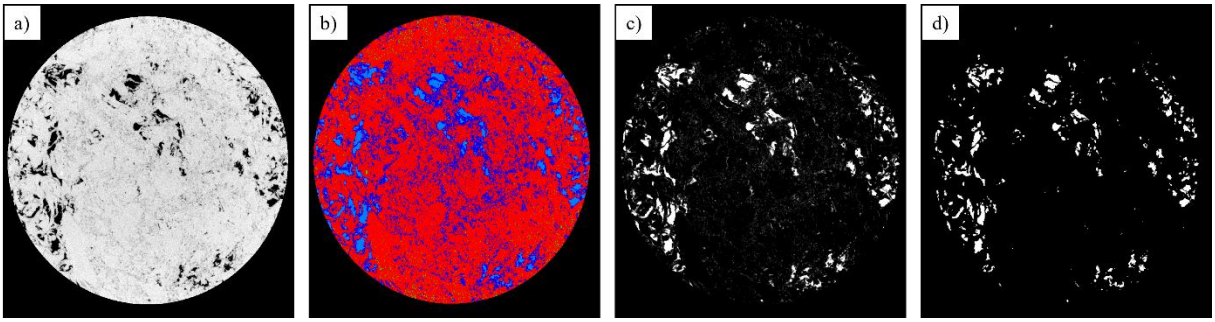


Figure 3. MicroCT slices of sample 141.0 (voxel size: 14 µm) showing processing steps for porosity and FFI: (a) grayscale image with pores in black and rock matrix in gray; (b) multiphase segmentation map showing resolved pores (light blue), sub-resolution porosity (dark blue), and solid material (red); (c) voxel-based pore percent image; (d) estimated FFI space after digital erosion.

Figure 4 compares the measured gas permeability with the values estimated by the Timur-Coates (TC) model applied to NMR data (a) and microCT data (b). Both methods show a general correlation trend with the experimental data, but with notable differences in accuracy and scatter. In Fig. 4a, the model based on NMR data performs better, with $R^2 = 0.756$ and Pearson correlation coefficient $r = 0.863$, indicating that the estimated permeability captures the variations among samples well. Nevertheless, some scatter around the 1:1 line (dashed line) is observed, especially at intermediate and high permeability values. This deviation may be related to limitations of NMR in distinguishing connected pores from isolated pores or to the empirical nature of the TC model.

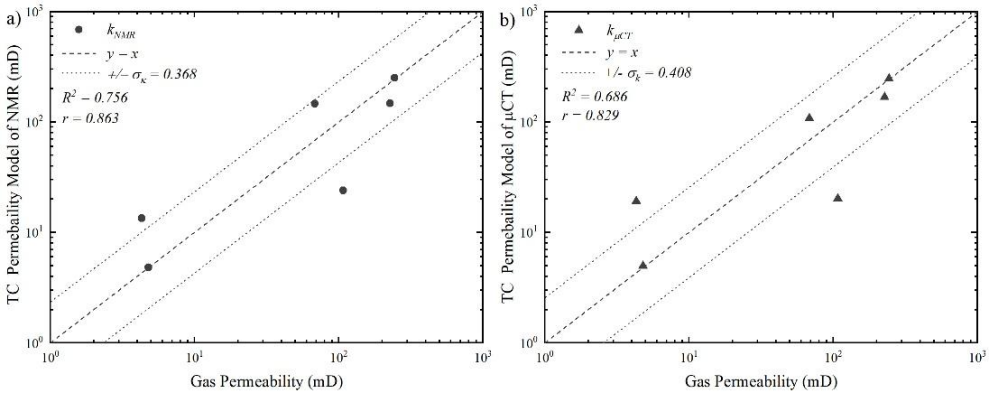


Figure 4. Cross-plots comparing gas permeability with the TC permeability model estimated to be from (a) NMR (circle) and (b) micro-CT (triangle). The dashed line represents the 1:1 reference line (y = x), and the dotted lines indicate $\pm\sigma_k$ error RMSLE.

In Fig. 4b, the model based on microCT data shows slightly lower performance ($R^2 = 0.686$; $r = 0.829$), with greater data scatter and a marginally higher Root Mean Squared Logarithmic Error (RMSLE) ($\sigma_k = 0.408$ compared to 0.368 for NMR). This can be attributed to the limited spatial resolution of microCT, which hampers the detection of smaller pores, as well as possible inaccuracies in binary segmentation (thresholding). It is also possible that the pore connectivity observed in the images does not fully reflect the effective gas flow paths under experimental conditions, especially when pores are partially saturated or capillary scaling effects are present.

4 Conclusions

This work presented an innovative and non-destructive methodology to estimate free fluid porosity (FFI) in hybrid carbonate rocks by applying digital erosion on segmented microCT images. The FFI estimated by microCT, after segmentation and digital erosion, showed consistent correlation with values obtained by NMR and was successfully used in the empirical Timur-Coates model to predict permeability. Permeability values estimated by

microCT ($R^2 = 0.686$; $r = 0.829$; $\sigma_k = 0.408$) were comparable to those obtained via NMR ($R^2 = 0.756$; $r = 0.863$; $\sigma_k = 0.368$), validating the potential of the image-based approach. Despite minor spatial resolution and segmentation differences, the integration of pore-scale imaging and petrophysical modeling proved robust. Furthermore, the correlation between pore size distributions obtained by microCT and NMR, calibrated by MICP, allowed estimation of an effective relaxivity parameter (ρ_e), essential for converting relaxation times into physical pore dimensions. The digital erosion technique enabled spatial delineation of the free fluid volume, distinguishing it from zones associated with irreducible fluid, thereby improving the accuracy of FFI quantification directly from image data. The results demonstrate that combining microCT image analysis with NMR in heterogeneous carbonate systems offers a reliable and scalable alternative to conventional methods. In reservoir studies, future applications may extend this methodology to larger datasets, multiphase flow simulations, and calibration of upscaling models from core to well log scale.

Acknowledgements. This research was carried out in association with the ongoing R&D projects registered as ANP 19027-2, “Desenvolvimento de infraestrutura para pesquisa e desenvolvimento em recuperação avançada de óleo – EOR no Brasil” (UFRJ/Shell Brasil/ANP) setting up an advanced EOR Laboratory facility for R&D in Brasil, and ANP 20163-2, “Análise experimental da recuperação de petróleo para as rochas carbonáticas do pré-sal brasileiro através da injeção alternada de CO2 e água”, with samples provided by Project SACL (Análise geológica sedimentar de sucessões carbonáticas do Cretáceo em uma bacia sedimentar brasileira (ANP n.18993-6), all sponsored by Shell Brasil under the ANP R&D levy as “Compromisso de Investimentos com Pesquisa e Desenvolvimento”. This study was financed in part by the Coordenação de Aperfeiçoamento de Pessoal de Nível Superior-Brasil (CAPES), Finance Code 001, and carried out with the support of CNPq, National Council of Scientific and Technological Development, Brazil. We acknowledge Professor Rodrigo Bagueira (UFF-LAR) for helping with saturating the samples and use of the NMR equipment. We also thank the research teams of LRAP/COPPE/UFRJ and LAGESED/UFRJ.

Authorship statement. The authors hereby confirm that they are the sole liable persons responsible for the authorship of this work, and that all material that has been herein included as part of the present paper is either the property (and authorship) of the authors or has the permission of the owners to be included here.

References

[1] N. Zhang, S. Wang, F. Zhao, X. Sun, M. He, “Characterization of the pore structure and fluid movability of coal-measure sedimentary rocks by nuclear magnetic resonance (NMR)”. ACS Omega 6:22831–22839, 2021.
[2] R. A. Victor. Multiscale, image-based interpretation of well logs acquired in a complex, deepwater carbonate reservoir. PhD thesis, The University of Texas at Austin, 2017.
[3] A. Mirshadi, A. Javaherian, M. Saberi, A. Kadkhodaie, H. Khoshdel, “Estimation of pore-type distribution utilizing petrophysical data and rock physics modeling on an Iranian carbonate reservoir”. J. Pet. Explor. Prod. Technol., 2024.
[4] G. Coates, M. Miller, M. Gillen, G. Henderson, “An investigation of a new magnetic resonance imaging log”. SPWLA conference in Midland, Texas, 1991.
[5] M. Lima, E. Pontedeiro, M. Ramirez, A. Boyd, M. Th. van Genuchten, L. Borghi, P. Couto, A. Raoof, “Petrophysical Correlations for the Permeability of Coquinas (Carbonate Rocks)”. Transport in Porous Media, 135, pp. 278-308.
[6] N. Azambuja, L. Arienti, F. Cruz, “Guidebook to the rift-drift Sergipe-Alagoas passive margin basin, Brazil”. In: AAPG Int. Conf. and Exhibition. AAPG, Rio de Janeiro, Brazil, pp. 11, 1998.
[7] O. A. Campos Neto, W. Souza-Lima, F. G. Cruz, “Bacia de Sergipe-Alagoas”. Boletim de Geociências da Petrobras, vol. 15, pp. 405–415, 2007.
[8] A. Tavares, L. Borghi, P. Corbett, J. Nobre-Lopes, R. Câmara, “Facies and depositional environments for the coquinas of the Morro do Chaves Formation, Sergipe-Alagoas Basin, defined by taphonomic and compositional criteria” Braz. J. Geol., 2015.
[9] E.W. Washburn, “The dynamics of capillary flow”. Physical Reviews, 1921.
[10] M. Fleury and M. Romero-Sarmiento, “Characterization of shales using T1–T2 NMR maps”. J. Petrol. Sci. Eng., 137, pp. 55–62, 2016.
[11] P. Mesquita, R. Azeredo, E. Rios, et al., “NMR-MICP Integration and Permeability: A new free petrophysics software”. IBP. In: Rio Oil and Gas Expo & Conference IBP-1370-16, 2016.
[12] S. Foroughi, B. Bijeljic, Y. Gao, M. Blunt, “Incorporation of Sub-Resolution Porosity Into Two-Phase Flow Models With a Multiscale Pore Network for Complex Microporous Rocks”. Water Resources Research, 60, 22023WR036393, 2024.
[13] R. Gonzalez and R. Woods, “Processamento de imagens digitais”. Editora Blucher, 2000.
[14] G. Coates, L. Xiao, M. Prammer, “NMR logging principles and applications”. Houston, Halliburton Energy Services, pp. 235, 1999.
[15] P. Silva, E. Gonçalves, E. Rios, A. Muhammad, A. Moss, et al., “Automatic classification of carbonate rocks permeability from ^{1}H NMR relaxation data”. Expert Systems with Applications, 42, pp. 4299–4309, 2015.